

**Mn²⁺ EPR study of phase transitions in dicalcium lead propionate Ca₂Pb(C₂H₅COO)₆:
Determination of critical exponent below the ferroelectric phase transition
and comparison with EPR studies on Ca₂Ba(C₂H₅COO)₆ and Ca₂Sr(C₂H₅COO)₆**

Sushil K. Misra and Stanislaw Jerzak

Physics Department, Concordia University, 1455 de Maisonneuve Boulevard West, Montreal, Quebec, Canada H3G 1M8

(Received 10 June 1988; revised manuscript received 22 August 1988)

The phase transitions undergone by DLP [dicalcium lead propionate Ca₂Pb(C₂H₅COO)₆] crystal have been studied via the EPR of Mn²⁺. Two phase transitions, one second order at 343±2 K and another first order at 180±2 K, have been deduced to occur, as revealed by the behavior of overall splitting of EPR lines and that of EPR linewidth. In the ferroelectric phase, below $T_{C1}=343$ K, the EPR spectra for the external magnetic field orientation in the {111}_C plane varies with temperature as $(T-T_{C1})^\beta$, where $\beta=0.51\pm 0.03$. The orientations of the magnetic Z axes corresponding to the various Mn²⁺ complexes above T_{C1} have been determined. As well, the temperature at which the high-temperature hypothetical phase transition to a cubic phase is supposed to take place, has been determined to be 490 K from the temperature variation of the overall splitting of lines for the magnetic field orientations along the magnetic Z and X axes. The Mn²⁺ spin-Hamiltonian parameters in Ca₂Pb(C₂H₅COO)₆ are evaluated above T_{C1} using a rigorous least-squares fitting procedure. The angular variation of the spectra reveals that the crystal structure is tetragonal both above and below $T_{C2}=180$ K. EPR linewidth variation with temperature has been studied to deduce the ordering of the propionate molecules surrounding the Mn²⁺ ion in the various phases, as well as the nature of phase transitions at T_{C1} and at T_{C2} . The present EPR studies are compared with those on Ca₂Sr(C₂H₅COO)₆ (dicalcium strontium propionate, DSP) and Ca₂Ba(C₂H₅COO)₆ (dicalcium barium propionate, DBP) in order to understand the systematics of the phase transitions and the ordering of ions surrounding Mn²⁺ ion in DBP, DSP, and DLP single crystals.

I. INTRODUCTION

Dicalcium lead propionate Ca₂Pb(C₂H₅COO)₆ (DLP hereafter) is paraelectric above 333 K with tetragonal crystal structure.¹ At $T_{C1}=333$ K it undergoes a second-order phase transition becoming ferroelectric below 333 K. As the temperature is decreased further, it undergoes a first-order phase transition at $T_{C2}=191$ K and still remains ferroelectric. It should be noted that the T_{C1} and T_{C2} values, mentioned in this section in context with the published results, are somewhat different from those determined in the present work as mentioned in the abstract and in the other sections of the paper. At all temperatures DLP is both ferroelastic and ferrogyrotropic. As for high temperatures, DLP is predicted to undergo a hypothetical phase transition, if it did not melt, to a cubic structure similar to that of dicalcium barium propionate Ca₂Ba(C₂H₅COO)₆ (DBP hereafter).² The mechanisms responsible for the various phase transitions which DLP goes through are still not fully understood, thereby attracting much interest in the phase-transition studies of it.

The ferroelectric phase transition at T_{C1} in DLP is believed to result from a mechanism similar to that responsible for the ferroelectric transition in dicalcium strontium propionate Ca₂Sr(C₂H₅COO)₆ (DSP hereafter) at 281 K, i.e., Pb-O-Ca interactions.^{3,4} Very little is known so far of the nature of the phase transition of DLP at T_{C2} . Gesi and Ozawa⁵ have suggested, on the basis of their hydrostatic pressure measurements, that the crystal structures of DLP and DSP above and below the respective

phase transitions are isomorphous to each other. Gesi,⁶ on the other hand, on the basis of polarizing-microscopic observations and dielectric constant measurements, has concluded that the two phases above and below T_{C2} are not isostructural.

There are no detailed x-ray structural data available for DLP crystal, and not much is known about its structural disorder. Dielectric,⁷ optical,⁸ and NMR⁹ studies of the ferroelectric transition of DLP at T_{C1} have been reported. Spontaneous polarization measurements of Takashige *et al.*⁸ revealed that DLP is ferroelectric below 333 K. Studies of pyroelectricity of DLP associated with its phase transitions by Osaka, Makita, and Gesi¹⁰ resulted in the conclusion that the DLP crystal between $T_{C1}=333$ K and $T_{C2}=193$ K is tetragonal and polar, the point group in this phase being C_4 or C_{4v} . Nagae *et al.*¹¹ studied the phase diagram of the mixed system Ca₂Pb_xSr_{1-x}(C₂H₅COO)₆ on the basis of dielectric and dilatometric anomalies. They confirmed that the space groups of DLP are D_4^4 (D_4^8) above T_{C1} and C_4^2 (C_4^4) below T_{C1} (at room and low temperatures). Nagae *et al.*¹² observed Raman scattering spectra of DSP and DLP between 73 and 423 K. They concluded that both the phase transitions of the two materials were of the order-disorder type since no soft modes were observed implying that the II-III transitions are most probably isomorphous. Piezoelectric and elastic properties of ferroelectric DLP were measured by Takashige¹³ over a wide temperature region including the ferroelectric-paraelectric phase-transition point (T_{C1}). The results were compared with those for DSP.

No detailed single-crystal EPR study has yet been reported of the phase transitions undergone by DLP. The only EPR study that has been reported on DLP is that by Bhat *et al.*¹⁴ However, their results are not significant. They only found that extra lines appear in powdered samples of DLP below the phase transition at T_{C2} . Detailed Mn^{2+} EPR studies of the phase transitions experienced by DBP and DSP crystals have already been reported.^{15,16}

It is the purpose of the present paper to report detailed studies of the phase transitions experienced by DLP crystals via the EPR of Mn^{2+} . To this end, the orientations of the magnetic Z axes of the various Mn^{2+} complexes in DLP above T_{C1} have been determined from detailed angular variations of EPR spectra for the orientation of the Zeeman field B in several planes. In addition, Mn^{2+} spin-Hamiltonian parameters above T_{C1} have been evaluated by the use of a rigorous least-squares-fitting procedure. In the ferroelectric phase it is possible to deduce the critical exponent β that governs the temperature variation of the angular splitting $\Delta\theta$ of the maxima of the overall splitting of Mn^{2+} EPR spectra [i.e., $\Delta\theta \propto (T - T_{C1})^\beta$] just below T_{C1} . Furthermore, the behavior of EPR linewidth as a function of temperature is studied in order to understand the ordering of molecules surrounding the Mn^{2+} ion in DLP crystal as well as the nature of the phase transitions at T_{C1} and T_{C2} . Finally, the present studies of DLP are compared with those of DBP and DSP crystals in order to understand the systematics of the phase transitions in DBP, DSP, and DLP crystals.

II. EXPERIMENTAL ARRANGEMENT AND SAMPLE PREPARATION

EPR spectra were recorded by the use of an X-band Varian V4506 spectrometer consisting of a 12-in. Varian electromagnet, a Varian power supply, and a Bruker field controller (B-NM-2). The crystal was placed inside a TE_{102} Varian cavity. Temperatures above and below room temperature were maintained at the sample by gently blown nitrogen gas passed through the heater coils, and coils immersed in liquid nitrogen, respectively, of a Varian temperature-controller unit (model E4540). The temperature stability was better than 0.5 K as measured by an Omega Engineering Inc. microprocessor-based thermocouple meter (model 680) with a temperature resolution of 0.1 K.

DLP crystals were grown by slow evaporation of an aqueous solution prepared by gradually dissolving PbO in an aqueous solution of propionic acid to which the calcium salt of propionic acid was added in stoichiometric proportion. The solution contained a sufficient amount of $MnCl_2$ so as to ensure that there was one Mn^{2+} ion per thousand Ca^{2+} ions. The best of the resulting crystals were dissolved in water for recrystallization. This process was repeated three times. In about three weeks, colorless DLP crystals of excellent quality were obtained. The crystal-growth habit of DLP is displayed in Fig. 1 which also exhibits the magnetic Z axes corresponding to the various Mn^{2+} complexes, as well as the cubic (C) and

tetragonal (T) axes.

Because the coordination numbers of both Ca^{2+} and Mn^{2+} are the same, i.e., six, and since the atomic radii of these two ions (0.80 Å for Mn^{2+} , 0.99 Å for Ca^{2+}) are also close to each other, it is expected that the Mn^{2+} ions substitute for Ca^{2+} ions. (On the other hand, the coordination number for Pb^{2+} ions is 12, while its atomic radius is 1.20 Å.) No detailed crystal structure is available for DLP crystal. However, analogous to DBP and DSP crystals, it is expected that the Ca^{2+} ions are surrounded by six oxygens of carboxyl groups of six different propionate molecules to form slightly distorted octahedra close in form to a trigonal antiprism, while the Pb^{2+} ions are surrounded by 12 equidistant carboxyl oxygens of six different propionate molecules.

Above T_{C1} , the crystal structure may be tetragonal, while between T_{C1} and T_{C2} it is tetragonal (either P_{41} or P_{43})³ with $a=b=12.50$ Å and $c=17.26$ Å. Below T_{C2} , the present measurements indicate a tetragonal crystal structure. Above and below T_{C2} , the particular point groups to which the tetragonal structures belong may be different. EPR spectra cannot determine this difference. This is known as isomorphous phase transition wherein the crystal structure does not change at the phase transition.

III. EPR SPECTRA IN THE PARAELECTRIC PHASE (373 K)

A. EPR spectra

Detailed angular variation of Mn^{2+} EPR spectra were recorded at 373 K in the paraelectric phase of DLP in order to determine the orientations of the magnetic Z axes corresponding to the various Mn^{2+} complexes in the unit cell of DLP. Because of the number of formula units per cell $Z=4$ analogous to DSP, there are expected to be eight Ca^{2+} sites in the unit cell of DLP. Of these, there

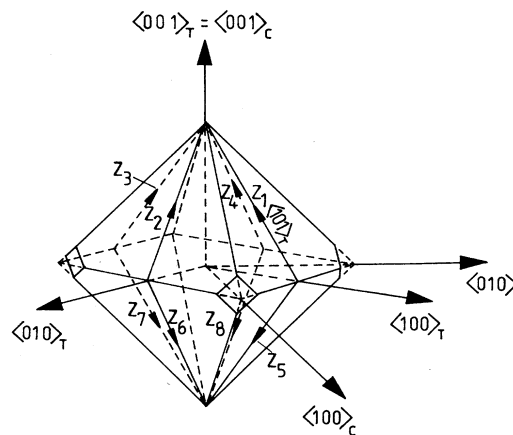


FIG. 1. Growth habit of DLP crystals (represented by solid lines). The cubic and tetragonal axes are indicated by the subscripts C and T , respectively. Note that $\langle 001 \rangle_T = \langle 001 \rangle_C$ and $\langle 101 \rangle_T = \langle 112 \rangle_C$. The various magnetic Z axes for Mn^{2+} are also exhibited.

are four sets of physically equivalent positions with two ions per set. (All of the four sets of Mn²⁺ ions in the unit cell are magnetically inequivalent.) Accordingly, four sets of physically distinct Mn²⁺ EPR spectra are observed for an arbitrary orientation of the external magnetic field. These spectra are identical to each other in every respect, except that their magnetic axes are differently oriented.

The angular variations of EPR spectra for the Zeeman field (**B**) orientations in the {100}_T and {111}_C planes are exhibited in Figs. 2 and 3, respectively. It has been found that the angular variations of EPR spectra for the orientation of **B** in the {010}_T plane is identical to that observed for **B** in the {100}_T plane. It can be seen from Fig. 2 that the absolute maximum of the overall splitting of lines occurs at ±33° from the <001>_C (= <001>_T) direction for **B** in the {100}_T plane; the same absolute maximum of overall splitting is observed to occur for **B** in the {111}_C plane along the median of the {111}_C face intersecting the <111>_C axis, i.e., along the {112}_C (= {101}_T) direction. The present observations reveal that the eight magnetic *Z* axes lie along the <112>_C, <112̄>_C, <11̄2>_C, <11̄2̄>_C, <112>_C, <11̄2̄>_C, <11̄2̄>_C, and <112̄>_C directions, that is, along the medians of the eight {111}_C-type faces passing through the <001>_C axis. (These are also coincident with <101>_T, <011>_T, <101̄>_T, <011̄>_T, <101̄>_T, and <011̄>_T, and constitute four pairs of physically different directions as well.) The orientations of the various *Z* axes are depicted in Fig. 1. As for the eight corresponding magnetic *X* axes which are defined as the directions of **B** for which the second maximum of overall splitting takes

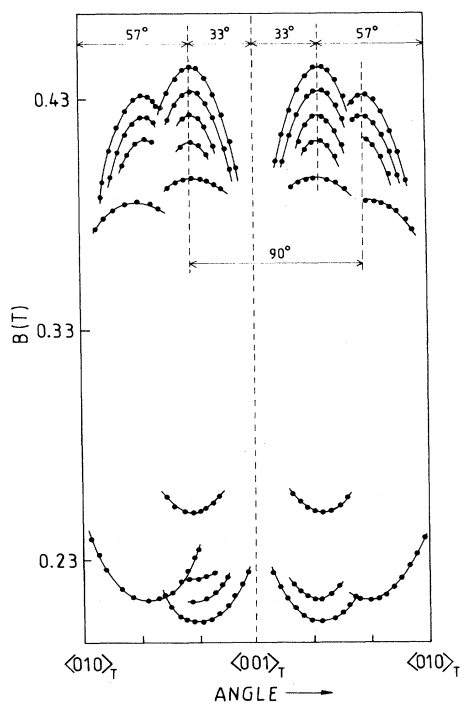


FIG. 2. Angular variation of Mn²⁺ EPR spectra in DLP at 373 K for **B** in the {100}_T plane.

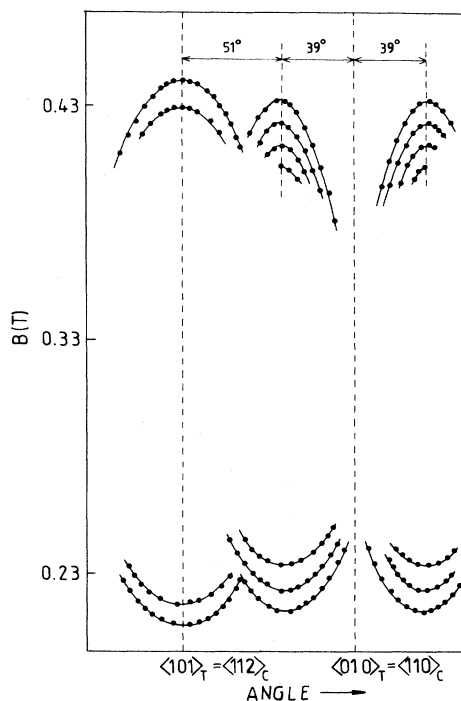


FIG. 3. Angular variation of Mn²⁺ EPR spectra in DLP at 373 K for **B** in the {111}_C plane.

place, they are found to be perpendicular to the <112>_C direction at an angle of 12° from the <111>_C and equivalent directions. Angular variation of EPR spectra for **B** in the {112}_C plane containing the magnetic *X* axis is exhibited in Fig. 4.

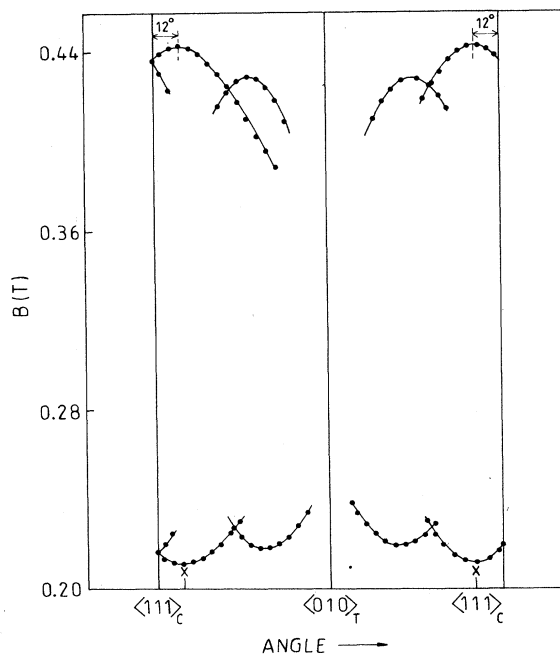


FIG. 4. Angular variation of EPR spectra for Mn²⁺-doped DLP at 373 K for the orientation of **B** in the {112}_C (= {101}_T) plane.

As for the two second maxima X'_1 and X'_2 that occur at 51° and 129° , respectively, for the $\langle 112 \rangle_C$ direction (Z axis) for \mathbf{B} in the $\{111\}_C$ plane (Fig. 3), they have been found, upon close examination, to correspond to the projections of the X axes, X_1 and X_2 , corresponding to the two other physically inequivalent Mn^{2+} ions whose respective Z axes are oriented along the medians of the faces adjoining the $\{111\}_C$ face and intersecting on the $\langle 001 \rangle_C$ axis, i.e., along the $\langle \bar{1}12 \rangle_C$ and $\langle 1\bar{1}2 \rangle_C$ directions. (X'_1 and X'_2 are found to be oriented rather close to X_1 and X_2 , respectively.)

The spectrum observed for $\mathbf{B} \parallel \langle 112 \rangle_C$ (i.e., the Z axis) is displayed in Fig. 5. It can be seen from this figure that the Mn^{2+} zero-field splitting parameter b_2^0 in DLP is sufficiently large so that the five hyperfine sextets can be clearly identified. This is helpful in the study of angular anisotropies at various temperatures, unlike that in the DSP crystal where the value of b_2^0 is rather small so that the five hyperfine sextets for DSP overlap each other considerably.

B. Spin-Hamiltonian parameters

The allowed ($\Delta M = \pm 1$, $\Delta m = 0$, where M and m are the electronic and nuclear quantum numbers, respectively) EPR line positions as observed at 373 K for \mathbf{B} in the ZX plane of any Mn^{2+} complex were fitted to the following spin-Hamiltonian (SH) appropriate to orthorhombic symmetry:

$$\begin{aligned} \mathcal{H} = & \mu_B [g_{\parallel} B_z S_z + g_{\perp} (B_x S_x + B_y S_y)] \\ & + (\frac{1}{3})(b_2^0 O_2^0 + b_2^2 O_2^2) + (\frac{1}{60})(b_4^0 O_4^0 + b_4^2 O_4^2 + b_4^4 O_4^4) \\ & + A S_z I_z + B (S_x I_x + S_y I_y) \\ & + Q' [I_z^2 - (\frac{1}{3})I(I+1)] + Q'' (I_x^2 - I_y^2). \end{aligned} \quad (3.1)$$

In Eq. (3.1), μ_B is the Bohr magneton, S ($=\frac{5}{2}$) and I ($=\frac{5}{2}$) are the Mn^{2+} electronic and nuclear spins, respectively, and O_j^m are spin operators as defined by Abragam and Bleaney.¹⁷ A rigorous least-squares-fitting (LSF) procedure¹⁸ utilizing numerical diagonalization of the SH

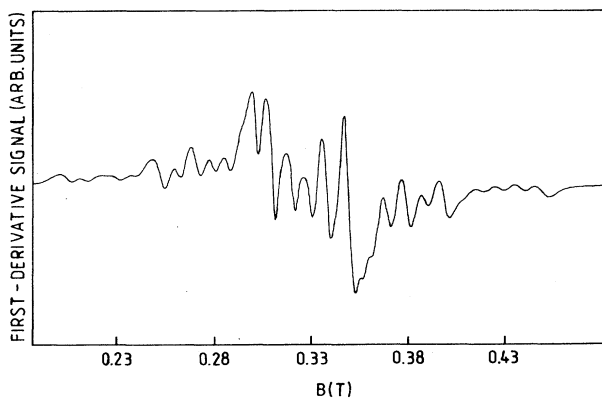


FIG. 5. X-band EPR spectrum for Mn^{2+} -doped DLP crystal at 373 K for \mathbf{B} along the magnetic Z axis ($\langle 101 \rangle_T$) of a Mn^{2+} complex. Note that $\langle 101 \rangle_T (= \langle 112 \rangle_C)$ is a bisector of the $\langle 111 \rangle_C$ face as shown in Fig. 1.

matrix on a digital computer in which all clearly resolved allowed line positions for a Mn^{2+} complex, observed the orientation of \mathbf{B} in its ZX plane, were simultaneously fitted to evaluate the nine SH parameters g_{\parallel} , g_{\perp} , b_2^0 , b_2^2 , b_4^0 , b_4^2 , b_4^4 , A , and B . The parameters Q' and Q'' could not be determined since the allowed line positions do not depend upon them. The errors of the parameters were determined by the use of a statistical method.¹⁹ Finally, a total of 55 line positions observed for \mathbf{B} in the ZX plane were used to evaluate the nine SH parameters. Generally, these included the three lowest-field lines of the first hyperfine (hf) sextet, the highest-field line of the fourth hf sextet, and the four highest-field lines of the fifth hf sextet for each of the orientations of \mathbf{B} close to the Z axis, and the two lowest-field lines of the first hf sextet, the highest-field line of the fourth hf sextet, and the three highest-field lines of the fifth sextet for each of the orientations of \mathbf{B} close to the X axis. (Here, the sextets are referred to in increasing values of the Zeeman field, i.e., the first hf sextet lies at the lowest values of \mathbf{B} while the fifth hf sextet lies at the highest values of \mathbf{B} .) The values of the SH parameters so evaluated are $g_{\parallel} = 2.006 \pm 0.001$, $g_{\perp} = 2.004 \pm 0.001$, $b_2^0 = 0.697 \pm 0.003$ GHz, $b_2^2 = -0.009 \pm 0.003$ GHz, $b_2^4 = -0.644 \pm 0.012$ GHz, $b_4^0 = -0.284 \pm 0.030$ GHz, $b_4^2 = 0.069 \pm 0.030$ GHz, $A = -0.270 \pm 0.004$ GHz, and $B = -0.269 \pm 0.006$ GHz. These values are characterized by the χ^2 value of 0.49 GHz². ($\chi^2 \equiv \sum [|\Delta E_j| - h\nu_j]^2$; here, ΔE_j is the calculated energy difference between the pair of levels participating in resonance for the j th line position, ν_j is the corresponding klystron frequency, and h is Planck's constant.) This implies an average difference of 0.1 GHz between the calculated separation of energy levels participating in resonance and the energy of microwave quantum (~ 9.5 GHz) per line. As for the absolute signs of the parameters, they could not be determined from the present data since no relative-intensity data were available at liquid-helium temperature. The sign of b_2^0 was then assumed to be positive. The signs of the other fine-structure parameters, relative to that of b_2^0 as yielded by the LSF procedure, are correct. The signs of the hyperfine parameters, A , B , were chosen to be negative in accordance with the hyperfine-interaction data.²⁰

C. Ferroelastic domains

In principle, three ferroelastic domains can exist in DLP:² I, II, and III, with their tetragonal axes parallel to the $\langle 100 \rangle_C$, $\langle 010 \rangle_C$, and $\langle 001 \rangle_C$ direction, respectively. The angular variation of EPR spectra for the variation of direction of \mathbf{B} in the $\{111\}_C$ plane confirms the existence of domain III only. Otherwise, in this angular variation, one should observe two other overall splittings: those for $\mathbf{B} \parallel \langle 211 \rangle_C$ and $\mathbf{B} \parallel \langle 121 \rangle_C$ corresponding to the domains with their tetragonal axes parallel to the $\langle 100 \rangle_C$ and $\langle 010 \rangle_C$ directions respectively, equal to that obtained for $\mathbf{B} \parallel \langle 112 \rangle_C$ direction. The existence of these maxima of overall splittings is not found as can be seen from the angular variation of spectra for \mathbf{B} in the $\{111\}_C$ plane (Fig. 3).

IV. HYPOTHETICAL PHASE TRANSITION TO CUBIC PHASE

Sawada *et al.*² have suggested that DLP, like DSP, should make a hypothetical transition from a tetragonal to a cubic phase at high temperatures. This cubic phase should actually be observed provided that the crystal does not melt before attaining this temperature. One expects that in the cubic phase the overall splittings $\Delta E(Z)$ and $\Delta E(X)$, observed for **B** along the *Z* and *X* axes, respectively, should become equal. In order to study this possibility, both $\Delta E(Z)$ and $\Delta E(X)$ were measured as functions of temperature and plotted in Fig. 6. It can be seen from Fig. 6 that both $\Delta E(Z)$ and $\Delta E(X)$ decrease linearly with increasing temperature, the decrease of $\Delta E(Z)$ being much greater than that of $\Delta E(X)$ so that the two become equal at about 490 K as found by extrapolation. The present measurements were carried out only up to 440 K since the crystal begins to deteriorate at temperatures above 440 K. No phase transitions of DLP have been detected by any other techniques above 400 K. The hypothetical tetragonal-cubic phase transition is expected to be an improper one as the mode responsible for it is the zone-boundary mode (the *X* point).²

V. CRITICAL BEHAVIOR OF THE PHASE TRANSITION BELOW T_{C1}

As the temperature was lowered through T_{C1} ($=343$ K), the DLP crystal experienced a phase transition of the second order from the paraelectric to the ferroelectric phase below T_{C1} . The critical behavior was exhibited by the temperature variation of θ representing the angular splitting of the maximum for **B** along the *Z* axis in the $\{111\}_C$ plane above T_{C1} which separated into two maxima, upon cooling through T_{C1} , and which were distributed symmetrically at $\pm\theta$ about the $\langle 112 \rangle_C$ direction for the variation of **B** in the $\{111\}_C$ plane. The angle θ describing this splitting is plotted as a function of temperature (*T*) in Fig. 7(a) while the corresponding log-log plot of θ versus *T* is exhibited in Fig. 7(b). A quantitative fit yields a variation of θ as

$$\theta = \theta_0(T_{C1} - T)^\beta, \quad (5.1)$$

where $\theta_0 = 1.148^\circ$ and $\beta = 0.51 \pm 0.03$.

The value of β thus obtained is consistent with that of a proper phase transition. Since, according to Landau's mean-field theory^{21,22} of second-order phase transitions, the order parameter *q* of the phase transition for proper transition varies as $(T_{C1} - T)^\beta$, where $\beta = 0.5$. For DLP, the spontaneous polarization P_s , which is a direct effect of the phase transition, is to be considered as representing the order parameter *q*. If P_s is measured by θ in the present case, then $P_s \propto (T_{C1} - T)^{0.5}$. [For improper transitions, P_s varies as q^2 , i.e., $P_s \propto (T_{C1} - T)$, since P_s , for this case, is a secondary effect of the phase transition manifested due to nonlinear coupling of P_s to *q*.] Furthermore, the present result ($\beta = 0.5$) is consistent with the spherical model for $d = 3$. As discussed by Misra and Shrivastara,²³ the exactly solvable spherical model for spatial dimension $d = 3$ yields the critical exponents $\beta = 0.5$, $\gamma = 2$, and $\delta = 5$.^{24,25}

It has been shown by Misra and Lewis^{26,27} that the polarization of the ions surrounding the paramagnetic ion determines the spin-Hamiltonian parameters, which, in turn, determine the orientations of the maxima of overall splitting of lines.²³ As the DLP crystal is cooled below T_{C1} , the ions surrounding Mn²⁺ become polarized thus destroying the physical pairwise equivalence of the eight Mn²⁺ ions in the unit cell prevalent above T_{C1} . This is

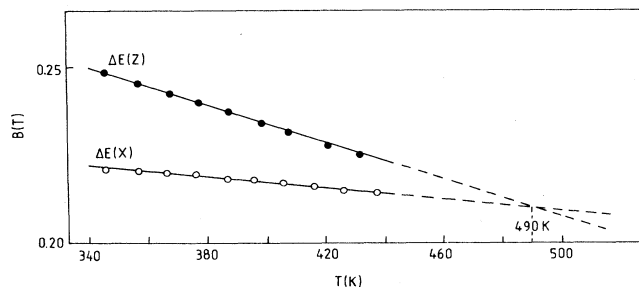


FIG. 6. Temperature variations of the overall splittings for Mn²⁺, $\Delta E(Z)$ and $\Delta E(X)$, for the orientation of **B** along the magnetic *Z* and *X* axes, respectively. It can be seen by extrapolation that $\Delta E(Z) = \Delta E(X)$ at about 490 K at which temperature the hypothetical phase transition to cubic structure is expected to occur.

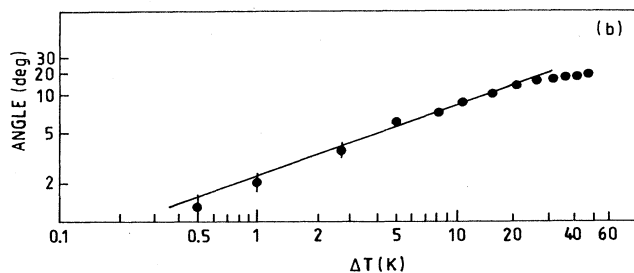
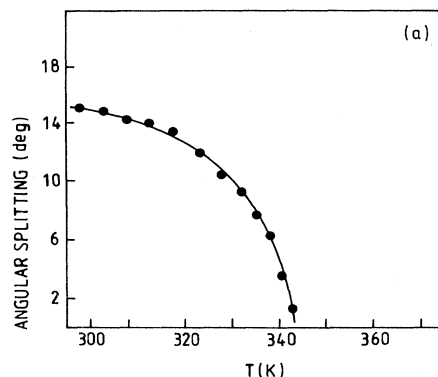


FIG. 7. (a) Temperature variation of the angular splitting, i.e., the angle at which either of the two maxima, into which the single maximum above 343 K splits below 343 K, shifts from the position of the single maximum above 343 K. (b) log-log plot below $T_{C1} = 343$ K of the angular splitting of maxima [as defined for (a)] vs the difference of temperature from 343 K.

responsible for the occurrence of two maxima below T_{C1} . Stadnicka *et al.*²⁸ proposed that the origin of the spontaneous polarization P_s in DSP crystal is the Sr-O-Ca interaction. It is likely that a similar mechanism, namely the Pb-O-Ca interaction, is effective in DLP crystal.

The angular splitting of maxima below T_{C1} is the most pronounced for **B** in the $\{111\}_C$ plane. Such splittings do take place for **B** in other planes also; however, they are not significantly large.

VI. PHASE TRANSITIONS

The features of EPR spectra and the behavior of EPR linewidths as functions of temperature can be used to deduce the occurrence of first-order and second-order phase transitions undergone by DLP. Figure 8 exhibits the position of the highest-field line for **B** at 17° from the median (Z axis) in the $\{111\}_C$ plane as a function of temperature in the range 315–370 K. This clearly shows the occurrence of a second-order phase transition at 343 K, as the slopes are different on the two sides of 343 K. On the other hand, Fig. 9 exhibits the EPR spectra as functions of temperature for **B** at 22° from the median (Z axis) in the $\{111\}_C$ plane in the range 177–218 K. The occurrence of a first-order phase transition at 180 ± 2 K can clearly be seen from this figure as there is an abrupt change in the features of the spectrum at this temperature. The behavior of EPR linewidth as a function of temperature is displayed in Fig. 10 from which it is clear that above and below $T_{C1} = 343 \pm 2$ K the features of the EPR linewidth are different from each other; the transition between these two phases is gradual as a function of temperature. On the other hand, it can be seen from Fig. 10 that the change of the linewidth between the two phases above and below $T_{C2} = 180 \pm 2$ K takes place in a drastic manner as a function of temperature. Thus, the linewidth behavior also confirms that at 343 ± 2 K and 180 ± 2 K, DLP undergoes second-order and first-order phase transitions, respectively. The phase transition at T_{C2} is found to be strongly first order in nature, as the

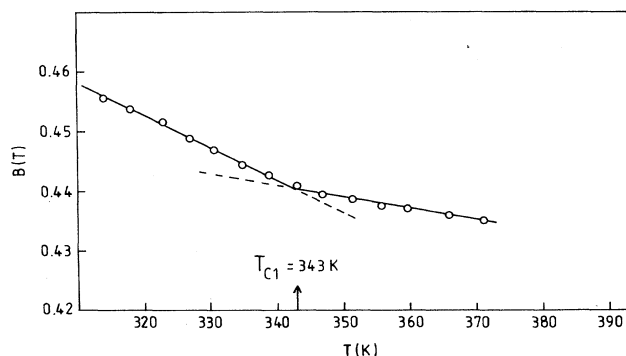


FIG. 8. Position of the highest-field Mn^{2+} EPR line in DLP observed for **B** at 17° from the Z axes in the $\{111\}_C$ plane over a temperature range covering $T_{C1} = 343$ K. It can be seen that the slopes are different on the two sides of 343 K although the line position does not shift abruptly at 343 K. This indicates that, at 343 K, DLP undergoes a phase transition of second order.

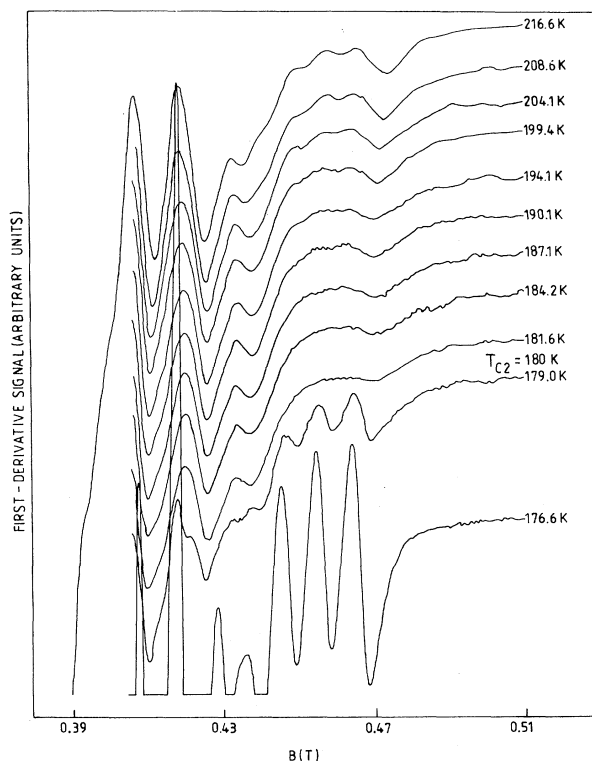


FIG. 9. Temperature variation of Mn^{2+} EPR spectra in DLP for **B** at 22° from the $\langle 112 \rangle_C$ direction in the $\{111\}_C$ plane over a temperature range covering $T_{C2} = 180$ K. It can be clearly seen that above and below 180 K the spectra are drastically different, implying the occurrence of a first-order phase transition in DLP at 180 K.

two phases above and below T_{C2} coexist over a narrow temperature range of about 2 K as can be seen from EPR spectra, and this transition is characterized by a temperature hysteresis of about 8 K.

VII. EPR SPECTRA BELOW T_{C1}

The details of the angular variations of the EPR spectra and those of the intensities in the two phases below T_{C1} ($= 333$ K), i.e., at 298 and at 173 K are described below.

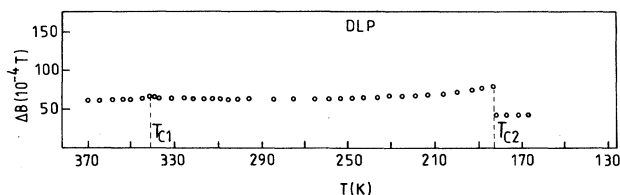


FIG. 10. Variation of Mn^{2+} EPR linewidth of the highest-field line in DLP as a function of temperature for **B** at 30° from the $\langle 101 \rangle_T$ ($= \langle 112 \rangle_C$) direction (Z axis) in the $\{111\}_C$ plane. Two phase transitions, a second order at $T_{C1} = 343 \pm 2$ K, and a first order at $T_{C2} = 180 \pm 2$ K, are clearly revealed by the behavior of the linewidth as a function of temperature.

A. 298 K

The angular variation of the EPR spectra for **B** in the $\{100\}_T$ and $\{111\}_C$ planes are depicted in Figs. 11 and 12, respectively. The angular variation of the spectra for **B** in the $\{100\}_T$ plane is found to be the same as that for **B** in the $\{010\}_T$ plane. This indicates that the crystal structure continues to remain tetragonal below T_{C1} . Furthermore, the angular variation of EPR spectrum for **B** in the $\{100\}_T$ plane (the same as that in the $\{010\}_T$ plane) at 298 K (Fig. 11) are not much different from the corresponding angular variations at 373 K, i.e., above T_{C1} (Fig. 2). As for the angular variation of EPR spectra for **B** in the $\{111\}_C$ plane (Fig. 12) at 298 K (i.e., below T_{C1}), it has been found to be significantly different from the corresponding angular variation at 373 K as displayed in Fig. 3 and as discussed in Sec. V. In particular, each maximum at 373 K splits into two maxima at 298 K. However, the intensities of these two sets of spectra are significantly different from each other; one set of lines (represented by continuous lines in Fig. 12) is much more intense while the other set of lines (represented by dotted lines in Fig. 12) is quite weak. (The peak-to-peak first-derivative heights of EPR lines represented by the solid lines are about five times those represented by the dotted lines in Fig. 12.)

B. 173 K

The angular variations of spectra at 173 K (i.e., below T_{C2}) for **B** in the $\{100\}_T$ and $\{111\}_C$ planes are exhibited in Figs. 13 and 14, respectively. The angular variation of spectra for **B** in the $\{010\}_T$ plane is identical to that for **B** in the $\{100\}_T$ plane indicating that the crystal structure continues to remain tetragonal even below T_{C2} . Furthermore, the angular variations of spectra for **B** in the $\{100\}_T$ and $\{111\}_C$ planes at 173 K (i.e., below T_{C2}) are more or less the same as those in the corresponding planes at 298 K, as can be seen by a comparison of Figs. 11 and 12 with Figs. 13 and 14, respectively. In particular, it is noted that the angular splitting of maxima for **B** in the $\{111\}_C$ plane is $2\theta=18^\circ$ at 173 K, while it is $2\theta=29^\circ$ at 298 K, changing abruptly at $T_{C2}=180$ K as the temperature is lowered. As for the relative intensities of the EPR lines corresponding to these maxima, it has been found that the lines, which are more intense (five times that of the other set) at 298 K ($< T_{C1}$) (as shown in

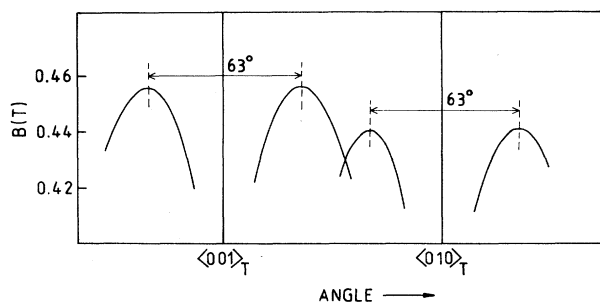


FIG. 11. Angular variation of Mn²⁺ EPR spectra in DLP at 298 K for **B** in the $\{100\}_T$ plane.

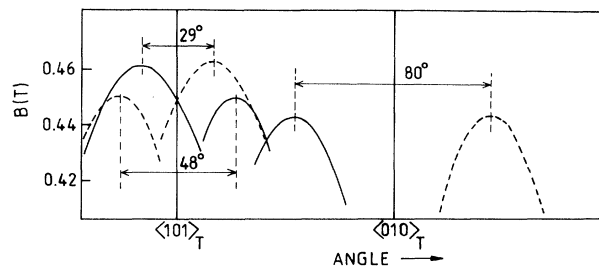


FIG. 12. Angular variation of Mn²⁺ EPR spectra in DLP at 298 K for **B** in the $\{111\}_C$ plane. The EPR lines represented by the solid lines have about five times the intensity of the symmetrically located lines represented by the dotted lines.

Fig. 12), are less intense (one-fifth that of the other set) at 173 K ($< T_{C2}$) (as shown in Fig. 14). (Here, the intensities are measured in terms of their peak-to-peak first-derivative line heights.)

VIII. LINEWIDTHS

It can be seen from Fig. 10 that below $T_{C2}=180\pm 2$ K, the linewidth which is independent of the orientation and magnitude of **B** at any temperature, drops to about 60% of its value representing the fact that below T_{C2} the propionate molecules surrounding the Mn²⁺ ion, whose carboxyl (COO) groups coordinate with the Mn²⁺ ion, become much more ordered than they are above T_{C2} because the range of sites available to the propionate molecules becomes much narrower below T_{C2} . On the other hand, when going below $T_{C1}=345\pm 5$ K but remaining above T_{C2} , only a partial ordering of propionate molecules may occur, thereby not affecting the linewidth significantly.

IX. CONTROVERSY ABOUT SYMMETRY CHANGE AT T_{C2} IN DLP

According to Gesi²⁹ the crystal symmetry of the DLP not change at the phase transition at T_{C2} , i.e., at T_{C2} DLP undergoes an isomorphous phase transition. This was further confirmed by Nagae *et al.*¹² by Raman scattering, and by Nagae *et al.*¹¹ by a study of the mixed crystals of DSP and DLP. Later, Gesi⁶ reinterpreted his

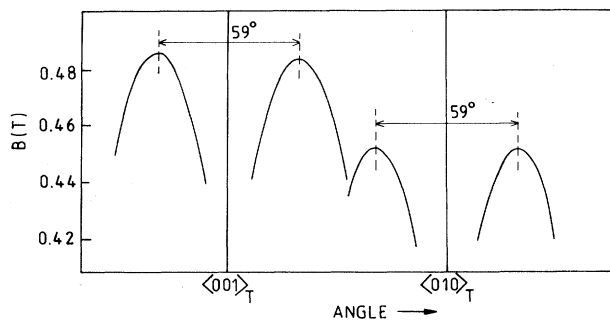


FIG. 13. Angular variation of Mn²⁺ EPR spectra in DLP at 173 K for **B** in the $\{100\}_T$ plane.

pressure measurements in DSP and DLP crystals taking into consideration the x-ray and microscopic studies of Hosokawa *et al.*³⁰ and the powder EPR studies of DSP and DLP by Bhat *et al.*¹⁴ who observed "new" EPR lines below T_{C2} . Hosokawa *et al.*³⁰ proposed a change of crystal symmetry from C_4 to C_2 (tetragonal to monoclinic) below T_{C2} . The present detailed single-crystal EPR study indicates that the EPR lines in DSP crystal¹⁶ are too broad to be observed below T_{C2} ; thus, the conclusion of Bhat *et al.*¹⁴ is doubtful. As for DLP, there is no additional splitting of lines observed below T_{C2} which should take place if the symmetry, indeed, changes from tetragonal to monoclinic. Only an abrupt reduction in the value of the angle 2θ , by which the maxima of EPR lines are separated from each other for **B** in the $\{111\}_C$ plane at T_{C2} , was observed. It is quite likely that the so-called "new" EPR lines observed by Bhat *et al.*¹⁴ in DLP below T_{C2} are not, indeed, new lines. They exist above T_{C2} but are not observable due to the fact that they are rather wide. They become observable because of increased line height caused by reduction in the linewidth below T_{C2} .

The symmetry of the angular variation of the EPR spectra of DLP remains the same above and below T_{C2} , while the relative intensities of the EPR lines above and below T_{C2} change. This implies that DLP undergoes an isomorphous transition at T_{C2} which is first order in nature and is accompanied by a change of the statistical weight accorded to the distribution of the possible configurations available to the molecules surrounding Mn^{2+} ion.

X. COMPARISON OF EPR STUDIES ON PHASE TRANSITIONS IN DBP, DSP, AND DLP CRYSTALS

It is interesting to examine the various EPR results on DBP, DSP, and DLP crystals in order to understand the systematics of the phase transitions in these dicalcium metal propionates.^{15,16}

A. Phase transitions

The hypothetical high-temperature phases of DSP and DLP are expected to be cubic, the same as that of DBP at

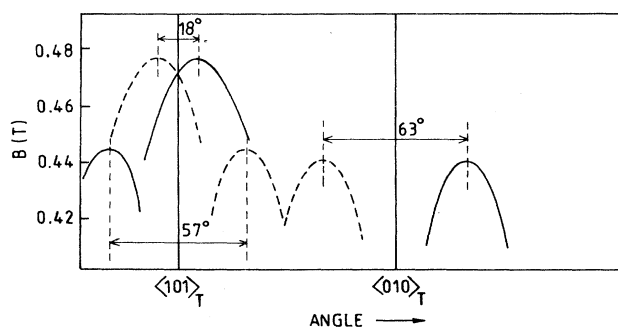


FIG. 14. Angular variation of Mn^{2+} EPR spectra in DLP at 173 K for **B** in the $\{111\}_C$ plane. The EPR lines represented by the solid lines have about five times the intensity of the symmetrically located lines represented by the dotted lines.

room temperature. Under high pressure, DBP is shown to behave similarly to DSP and DLP.^{1,31} As the temperature is lowered below room temperature, the DBP crystal undergoes a first-order phase transition at about 267 K and then a second-order phase transition at 207 K.^{1,2,15,16} If the succession of the phase transitions is to be compatible in the three crystals—DBP, DSP, and DLP—it would appear that, if they were not to melt at high temperatures, the sequence of the crystal structures of the phase transitions, as the temperature is decreased from the present EPR measurements on the three crystals, could be expected to be as follows.

I order II order I order
Cubic \leftrightarrow tetragonal \leftrightarrow tetragonal \leftrightarrow tetragonal ,

provided that DSP and DLP crystals do not melt at high temperatures. DSP and DLP become ferroelastic below the cubic \leftrightarrow tetragonal phase-transition temperature; also these two become ferroelectric below the second-order tetragonal \leftrightarrow tetragonal phase transition as well.

B. EPR spectra and orientations of the magnetic axes of Mn^{2+}

In the high-temperature hypothetical cubic phases of DSP and DLP the magnetic **Z** axes for Mn^{2+} are expected to be along the $\langle 111 \rangle_C$ or equivalent directions, the same as those found for DBP at room temperature in the cubic phase. Below the transition temperature to the hypothetical cubic phases, e.g., at 295 and 373 K, the magnetic **Z** axes for the various physically inequivalent Mn^{2+} complexes are oriented along the $\langle 101 \rangle_C$ and $\langle 112 \rangle_C$ or equivalent directions for DSP and DLP crystals, respectively, while the corresponding **X** axes are oriented very close to the $\langle 111 \rangle_C$ or equivalent directions. (The deviations are $\sim 4^\circ$ and $\sim 12^\circ$ for DSP and DLP in the $\{011\}_T$ and $\{112\}_C$ planes, respectively.) As the temperature is raised above the respective hypothetical phase-transition temperatures, the overall splittings of lines for **B** along the **Z** axis for DSP and DLP tend to become equal to those along the respective magnetic **X** axes in the two crystals predicting the occurrences of hypothetical phase transitions to cubic structures, with the magnetic **Z** axes being oriented along the $\langle 111 \rangle_C$ or equivalent directions for both DSP and DLP. Here it should be noted that the Mn^{2+} **Z** axes most likely correspond to trigonal distortion of CaO_6 octahedra in DSP and DLP crystals.

As for the Mn^{2+} EPR spectra, it is noted that DBP, in its cubic phase, exhibits axially symmetric spectra around the magnetic Mn^{2+} **Z** axes. On the other hand, the EPR spectra for DSP and DLP below the (hypothetical) cubic phase, i.e., at 298 and 373 K, respectively, exhibit spectra of orthorhombic symmetry; however, the orientations of the Mn^{2+} **Z** axes for DSP and DLP are not coincident. Unfortunately, the detailed crystal structure of DLP at 373 K, as determined from x-ray data, is not known; this makes it impossible to understand the reason for this difference.

C. EPR linewidths and ordering of propionate molecules

The behavior of the linewidth of the highest-field sextet for $B \parallel \hat{Z}$ as a function of temperature indicates that for

both DBP and DLP crystals there is a sharp drop in the linewidth as the temperature is decreased at the first-order phase transition, while this change is continuous at the second-order phase transition. (The sharp drop at the first-order phase transition for DSP is not observed. Instead, the lines corresponding to the noncentral sextets become too wide below the first-order phase transition for DSP to be observed experimentally.) The most important conclusion that can be drawn from this observation is that below the first-order phase-transition temperature, the propionate molecules surrounding the Mn²⁺ ion become much more significantly ordered than they are above this temperature in DBP and DLP. On the other hand, below the second-order phase transition temperature, only partial ordering of the propionate molecules is expected in DBP and DLP. This is in agreement with the x-ray results of Glazer *et al.*³ and those of Mishima.⁴ As for DSP, partial ordering of propionate molecules below the second-order phase transition temperature does, indeed, take place; however, below the first-order phase transition temperature there are several off-center positions available to the Mn²⁺ ion in the surrounding CaO₆ cage; this results in a distribution of the crystal field at the Mn²⁺ site which causes broadening of hf lines corresponding to the noncentral sextets.¹⁶

Table I lists the linewidths of the three highest-field sextets for DBP, DSP, and DLP for B||Z at 295, 295, and 373 K, respectively. (The larger errors in Table I are due to overlap by other lines.) An examination of Table I reveals that, in general, the linewidths in DBP and DSP are about the same, and significantly smaller than those in DLP. This may be attributed to the relative sensitivities of Mn²⁺ ions to the disorder of the surrounding propionate molecules in the three crystals since the Mn²⁺ ions are coordinated to the oxygens of the carboxyl group of the propionate molecules.

Another source of linewidth could be the M-O-Ca interaction; M=Sr and Pb in DSP and DLP crystals, respectively. The EPR linewidths in DLP are greater than those in DSP because this interaction is greater in DLP than in DSP. The greater strength of the interaction in DLP is also responsible for the higher phase-transition temperature T_{C2} in DLP (343 K) than that in DSP (298 K) since greater thermal energy is needed in DLP to overcome this interaction to trigger the phase transition.

D. Zero-field splitting

The values of the zero-field splitting parameters b_2^0 in DBP, DSP, and DLP crystals at 298, 298, and 373 K, respectively, are 0.391, 0.141, and 0.697 GHz. These

TABLE I. Mn²⁺ EPR linewidths (in gauss) as observed in the host crystals DBP, DSP, and DLP at 295, 295, and 373 K, respectively. Large errors result from overlap of lines by other lines.

Host	SEXTET		
	$\frac{5}{2} \leftrightarrow \frac{3}{2}$	$\frac{3}{2} \leftrightarrow \frac{1}{2}$	$\frac{1}{2} \leftrightarrow \frac{1}{2}$
DBP	31±3	25±3	21±3
DSP	26±3	22±3	18±2
DLP	61±6	45±6	34±5

values can be explained to be due to the interaction of the Mn²⁺ ion with the oxygens of the carboxyl groups of the surrounding propionate molecules. According to the point-charge model, $b_2^0 \propto r^{-5}$, where r is the average distance between the paramagnetic and the ligand ions. The average Ca-O distance in DBP (Mn²⁺ replaces Ca²⁺) as given by Glazer *et al.*³ is equal to 2.253 Å, while in DSP it is, on the average, 2.318 Å (ranging from 2.278 to 2.359 Å). The Ca-O distances in DLP crystal are unknown; however, the present b_2^0 value for DLP implies that they should be much smaller than those in DBP and DSP crystals.

E. Ferroelastic domains

The crystals used for the present EPR studies reveal the existence of only one ferroelastic domain: namely, the domain with its tetragonal axis parallel to the $\langle 001 \rangle_C$ direction in all three crystals.

XI. CONCLUDING REMARKS

The present EPR study of DLP along with those of DBP and DSP have helped in the understanding of the systematics of the phase transitions in these crystals. The splitting of the EPR spectra in DLP due to polarization of the surrounding molecules has been used to determine the critical exponent β ($=0.51 \pm 0.03$). Supplementary detailed studies using other techniques, e.g., x-ray, specific heat, NMR, Raman, calorimetric, and dilatometric measurements, are required for a complete understanding of the structural changes in DBP, DSP, and DLP crystals as they go through the various phase transitions.

ACKNOWLEDGMENTS

The authors are grateful to the Natural Science and Engineering Research Council of Canada for financial support (Grant No. A4485). The facilities of the Concordia University Computer Centre were used to evaluate the spin-Hamiltonian parameters reported in this paper.

¹*Ferroelectric and Related Substances*, Vol. 16 of *Landolt-Bornstein Scenes*, edited by T. Mitsui and E. Nakamura (Springer-Verlag, Berlin, 1982), Pt. B, pp. 217–22; Y. Ishibashi, T. Kikugawa, and A. Sawada, *J. Phys. Soc. Jpn.* **47**, 339 (1979), and references therein.

²A. Sawada, Y. Ishibashi, and Y. Takagi, *J. Phys. Soc. Jpn.* **43**, 195 (1977).

³A. M. Glazer, K. Stadnicka, and S. Singh, *J. Phys. C* **14**, 5011 (1981).

⁴N. Mishima, *J. Phys. Soc. Jpn.* **53**, 1062 (1984).

⁵K. Gesi and K. Ozawa, *J. Phys. Soc. Jpn.* **39**, 1026 (1975).

⁶K. Gesi, *J. Phys. Soc. Jpn.* **53**, 1602 (1984).

⁷N. Nakamura, H. Suga, H. Chihara, and S. Seki, *Bull. Chem. Soc. Jpn.* **38**, 1779 (1965).

- ⁸M. Takashige, H. Iwamura, S. Hirotsu, and S. Sawada, *J. Phys. Soc. Jpn.* **38**, 904 (1975).
- ⁹H. Shiraki, I. Tatsuzaki, and T. Yagi, *Phys. Status Solidi A* **7**, 227 (1971).
- ¹⁰T. Osaka, Y. Makita, and K. Gesi, *J. Phys. Soc. Jpn.* **38**, 292 (1975).
- ¹¹Y. Nagae, Y. Ishibashi, Y. Takagi, and H. Kameyama, *J. Phys. Soc. Jpn.* **41**, 1300 (1976).
- ¹²Y. Nagae, M. Wada, Y. Ishibashi, and Y. Takagi, *J. Phys. Soc. Jpn.* **41**, 1659 (1976).
- ¹³M. Takashige, S. Hirotsu, S. Sawada, and K. Hamano, *J. Phys. Soc. Jpn.* **45**, 558 (1978).
- ¹⁴S. V. Bhat, V. Dhar, and R. Srinivasan, *Ferroelectrics* **40**, 49 (1982).
- ¹⁵S. K. Misra and S. Jerzak, *Solid State Commun.* (to be published).
- ¹⁶S. K. Misra and S. Jerzak, *Solid State Commun.* (to be published).
- ¹⁷A. Abragam and B. Bleaney, *Electron Paramagnetic Resonance of Transition Ions* (Clarendon, Oxford, 1970).
- ¹⁸S. K. Misra, *Physica* **B121**, 193 (1983); *J. Magn. Reson.* **23**, 403 (1976).
- ¹⁹S. K. Misra and S. Subramanian, *J. Phys. C* **15**, 7199 (1982).
- ²⁰A. Steudel, *Hyperfine Interactions* (Academic, New York, 1970), p. 182.
- ²¹G. A. Smolenski, V. A. Bokov, V. A. Isupov, N. N. Krainik, R. E. Pasynkov, and A. I. Sokolov, in *Ferroelectrics and Related Materials*, edited by G. A. Smolenski (Gordon and Breach, New York, 1984).
- ²²M. E. Lines and A. M. Glass, *Principles and Applications on Ferroelectrics and Related Materials* (Clarendon, Oxford, 1973).
- ²³S. K. Misra and K. N. Shrivastava, *Phys. Rev. B* **33**, 2255 (1988).
- ²⁴M. Wortis, in *Proceedings of the Conference on Renormalization Group, Chestnut Hill, Pennsylvania, 1973*, edited by J. D. Gunton and M. S. Green (Temple University Press, Philadelphia, 1973), p. 96.
- ²⁵G. A. Baker, Jr., H. E. Gilbert, J. Eve, and G. S. Rushbrooke, *Phys. Rev.* **176**, 739 (1967).
- ²⁶N. R. Lewis and S. K. Misra, *Phys. Rev. B* **25**, 5421 (1982).
- ²⁷N. R. Lewis and S. K. Misra, *Phys. Rev. B* **27**, 3425 (1983).
- ²⁸K. Stadnicka, A. M. Glazer, S. Singh, and J. Sliwinski, *J. Phys. C* **15**, 2577 (1982).
- ²⁹K. Gesi, *J. Phys. Soc. Jpn.* **40**, 483 (1976).
- ³⁰T. Hosokawa, J. Kobayashi, Y. Ursu, and H. Miyazaki, *Ferroelectrics* **20**, 201 (1978).
- ³¹K. Gesi and K. Ojawa, *J. Phys. Soc. Jpn.* **38**, 467 (1975).